A New Transformer Model with Separate Common-Mode and Differential-Mode Capacitance

Østergaard, Christian; Kjeldsen, Claus; Nymand, Morten

Published in:
Proceedings - IECON 2020

DOI:
10.1109/IECON43393.2020.9255142

Publication date:
2020

Document version:
Accepted manuscript

A New Transformer Model with Separate Common-Mode and Differential-Mode Capacitance

Christian Østergaard
SDU Electrical Engineering
University of Southern Denmark
Odense, Denmark
choe@mci.sdu.dk

Claus Kjeldsen
SDU Electrical Engineering
University of Southern Denmark
Odense, Denmark
clk@mci.sdu.dk

Morten Nymand
SDU Electrical Engineering
University of Southern Denmark
Odense, Denmark
mny@mci.sdu.dk

***Abstract*—A new transformer equivalent circuit model is presented containing separate common-mode and differential-mode capacitors, allowing for direct and simple analysis of the transformers influence. The representation of common-mode and differential-mode signals in two-winding transformers have been described and presented. Problems related to two commonly used transformer equivalent circuit models are shown. Operation scenarios of an isolated full bridge phase-shift DC/DC converter is used to compare the new transformer model with a commonly used model. Three transformers with different turns-ratio are constructed, with the purpose of evaluating the transformer models. Both models provided accurate impedance prediction for transformers with turns-ratio equal to one. However, for turns-ratios different from one, the commonly used model has an error of 40%-132% in the predicted equivalent capacitance of the measurements, whereas the proposed model only has an error of 0.6%-7.3%. The proposed model is therefore the only model that predicts accurate transformer behavior for any turns-ratio.**

***Index Terms*—Common mode, Differential mode, Parasitic capacitance, Equivalent circuits, Transformers, Modeling, DC-DC power converters, Phase shifted converter, Impedance measurement**

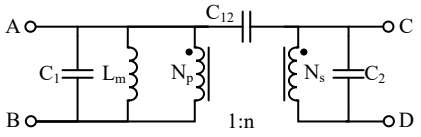

Fig. 1. The asymmetrical transformer model, excluding leakage inductance and winding resistance

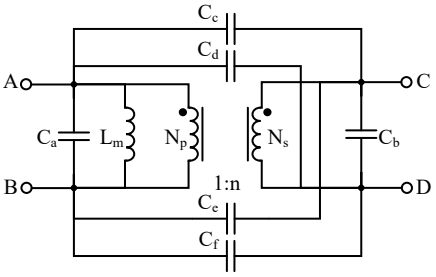

Fig. 2. The six-capacitor transformer model, excluding leakage inductance and winding resistance

I. Introduction

The equivalent circuit model of the transformer is a key factor in many aspects of a Switch-Mode Power Supply (SMPS) design, such as power loss calculation, common-mode (CM) and differential-mode (DM) filter design. An important element when designing a CM or DM filter is the amount of capacitance charged or discharged by the respective signals [1], [2]. The transformer models that currently exist does not clearly distinguish between whether the lumped capacitors are influenced by CM or DM signals, which is shown later in this paper. This makes it difficult to design proper filters for the SMPS.

Many different equivalent circuit models of the transformer has been presented in the literature. Common for all the models is that they contain an ideal transformer, windings resistances, capacitors, magnetizing and leakage inductances. When comparing the many different transformer models, it becomes clear that the main difference are the number and placement of the lumped capacitors. Two of the most commonly used transformer models are the asymmetrical three capacitor transformer model (henceforth called the asymmetrical model) [3]–[7] and the six-capacitor transformer model [8]–[12]. The two models are shown on Fig. 1 and Fig. 2 respectively, where the leakage inductance and winding resistance are excluded for the sake of simplicity.

The transformer model lumped circuit parameters is extracted from the measured transformer impedance in specific scenarios [6]–[8]. The specific scenarios does not always match the operation scenarios that the transformer is exposed to. Therefore the model should both be able to extract its equivalent circuit parameters from measurements, but also be able to predict the impedance in scenarios that have not been measured. Otherwise problems may arise when analyzing the transformer performance in operation scenarios of a SMPS.

The six-capacitor transformer model are widely used, because it has been shown to precisely depict the impedance of the transformer. The reason for its precision is that the parameters are determined by measuring the transformer in many different scenarios [8]. The model does however have at least two problems. The first problem lies in defining the amount of charge or discharge that comes from CM or DM

TABLE I
VOLTAGE POTENTIALS BETWEEN THE TRANSFORMER TERMINALS

Terminal voltage	Voltage equation
$V_A - V_B$	V_{dif}
$V_A - V_C$	$V_{com} + V_{dif}\ (1-n)\ /2$
$V_A - V_D$	$V_{com} + V_{dif}\ (1+n)\ /2$
$V_B - V_C$	$V_{com} - V_{dif}\ (1+n)\ /2$
$V_B - V_D$	$V_{com} - V_{dif}\ (1-n)\ /2$
$V_C - V_D$	$n\,V_{dif}$

signals, as multiple capacitors are affected by both signals. The second problem is the complexity of measuring the parameters, as it require specific measurements to have three resonance frequencies. Since transformer optimization typically leads to lowered parasitic parameters [13], the impedance resonances occurs at larger frequencies. Therefore, in certain cases are the resonances so numerically high in value that only the first resonance is visible and the rest is obscured by the non-modeled influences on the transformer.

The asymmetrical model is simpler than the six-capacitor model, mainly due to the lower number of lumped capacitors in the model. The asymmetrical model only needs the first resonance of the impedance measurement to determine the lumped capacitors. However, the asymmetrical model also has the problem of not being able to separate the amount of charge or discharge that comes from either CM or DM. Furthermore, it does not correctly mimic the measured transformer impedance for certain scenarios, which is proven later in the paper.

A new accurate equivalent circuit capacitance model of the transformer are therefore needed, which preferably is simple like the asymmetrical model, but also correctly mimics the transformer impedance. It should furthermore be able to clearly separate the amount of charge or discharge that comes from CM and DM signals In this paper, a new accurate transformer capacitance model is proposed which satisfies the previously mentioned conditions.

II. CM AND DM SIGNALS IN A TRANSFORMER

Fig. 3 is used to explain the CM and DM signals of a transformer. The figure illustrates a transformer with a turns-ratio of n, where signals are applied to each primary terminal (A and B), while each secondary terminal (C and D) are loaded with infinite impedance. All of the terminals signals V_A, V_B, V_C and V_D are referred to the same reference frame. The transformer CM signal (V_{com}) is defined as the difference between the CM level on either side of the transformer, whereas a DM signal in a transformer (V_{dif}) is defined as the difference between the primary terminals

$$V_{com} = (V_A + V_B)\ /2 - (V_C + V_D)\ /2 \tag{1}$$

$$V_{dif} = V_A - V_B \tag{2}$$

For the sake of simplicity is it assumed that the transformer model is loss-less, meaning that V_{dif} is transferred directly as a function of the turns-ratio. The DM signal on the secondary side is therefore

$$n\,V_{dif} = V_C - V_D \tag{3}$$

It is clear to see that any lumped capacitor placed between the transformer terminals A and B or C and D only experiences a pure DM signal. Capacitors placed between any other terminals are influenced by a mixture of CM and DM signals. For instance the voltage between terminal A and C are expressed as

$$\begin{aligned} V_A - V_C &= ((V_A + V_B) - V_B) - ((V_C + V_D) - V_D) \\ &= V_{com} + (V_A - V_B)\ /2 - (V_C - V_D)\ /2 \\ &= V_{com} + V_{dif}\ (1-n)\ /2 \end{aligned} \tag{4}$$

Table I lists all the possible combinations of voltage potentials between the transformer terminals, expressed in the form of V_{com} and V_{dif}. This shows that some of the capacitors in the six-capacitor and asymmetrical model are influenced by a mixture of CM and DM signals.

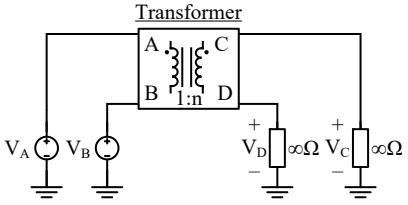

Fig. 3. Universal transformer application

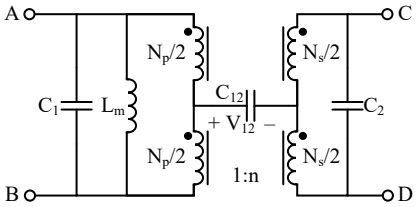

Fig. 4. The proposed symmetrical transformer equivalent circuit model, excluding leakage inductance and winding resistance

III. PROPOSED TRANSFORMER EQUIVALENT CIRCUIT CAPACITOR MODEL

A new equivalent circuit models of the transformer is proposed in which the lumped capacitors only is affected by either CM or DM signals. The proposed symmetrical model is shown on Fig. 4, where the leakage inductance and winding resistance are excluded. In the proposed model, both the primary and secondary winding of the ideal transformer, are split in two equal portions. This allows for the placement of C_{12} such that only the CM signal affects it. The split windings are all coupled to the same core, meaning half the primary voltage is across each portion of the primary winding, and half the secondary voltage is across each portion of the secondary winding. This representation of the ideal transformer provide the same analytical results as the ideal transformer used on the six-capacitor and asymmetrical model. The voltage signal V_{12}

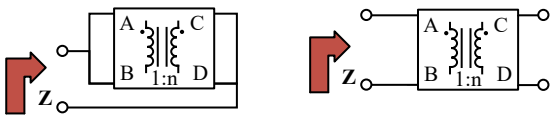

(a) Measure C_{12} (b) Measure L_m, C_1 and C_2

Fig. 5. Measurement method for extracting the transformer equivalent circuit parameters, L_m, C_1, C_2 and C_{12}

across the capacitor C_{12} in the symmetrical model are defined as

$$\begin{aligned} V_{12} &= (V_B + (V_A - V_B)/2) - (V_D + (V_C - V_D)/2) \\ &= (V_A + V_B)/2 - (V_C + V_D)/2 \\ &= V_{com} \end{aligned} \tag{5}$$

A. Extraction of the equivalent circuit parameters

It is described how to measure the asymmetrical model circuit parameters in [6]. The same method also applied for the symmetrical model. Two different measurements are needed to determine the values, one measurement extracting C_{12} and a measurement that determines L_m, C_1 and C_2.

The extraction of C_{12} is done by measuring the impedance between the primary and secondary side, where terminals A and B are shorted and terminals C and B are shorted, see Fig. 5a. The impedance of the asymmetrical and symmetrical models in this scenario are

$$Z_{CM} = \frac{1}{sC_{12}} \tag{6}$$

The parameters L_m, C_1 and C_2 is determined either by measuring the open circuit impedance on either the primary side or the secondary side. Fig. 5b shows the measurement of the primary side open circuit impedance. The impedance of the asymmetrical and symmetrical models in this scenario are

$$Z_{DM} = \frac{sL_m}{s^2 L_m \left(C_1 + n^2 C_2\right) + 1} \tag{7}$$

The measured equivalent capacitance in this scenario is $C_{eq} = C_1 + n^2 C_2$, which determines the joint capacitor values of C_1 and C_2. Additional measurements are needed to separate C_1 and C_2, however this is only possible if the leakage inductance and winding resistance is included. It should however be mentioned that it is not necessary to separate C_1 and C_2 for the following explanation.

IV. Operation of the transformer in a DC/DC converter

An isolated full bridge phase-shift DC/DC converter as shown on Fig. 6 is utilized to show the CM and DM signals in a transformer during normal operation. The converter operation is descried in [14]. For the sake of simplicity it is assumed that the voltage difference between primary and secondary return is zero ($V_G = 0$), as is often the case in SMPS. The CM and DM signals in the transformer during one switching

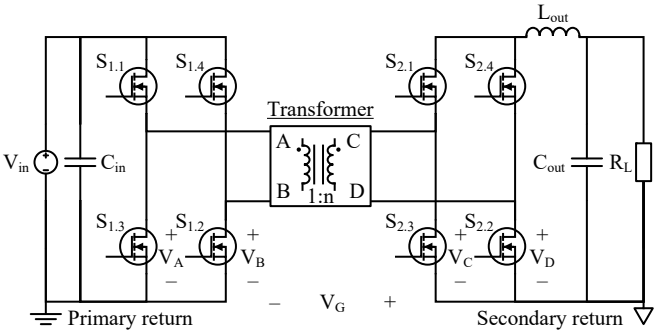

Fig. 6. Isolated full bridge phase-shift DC/DC converter

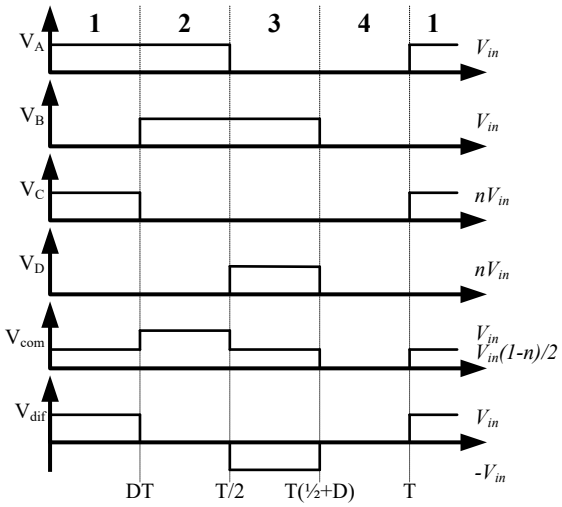

Fig. 7. Operation of an isolated full bridge phase-shift DC/DC converter

cycle is illustrated on Fig. 7, along with the voltage potentials at each of its four terminals.

The converter has four different operation scenarios during one switching cycle, as indicated by the numbers 1, 2, 3 and 4 on Fig. 7. Scenarios 1 and 3 are the power transfer states of the converter, in which the transformer is subjected to both CM and DM signals. Scenarios 2 and 4 are the free wheeling states of the converter. The transformer is only affected by a CM signal in scenario 2, whereas in scenario 4 no signal is applied to the transformer.

The circuitry involving the transformer during the four operation scenarios can be simplified as shown on Fig. 8, by assuming that the switches are ideal, meaning zero impedance when ON and infinite impedance when OFF. The dashed lined in each of the figures indicate a virtual short between primary and secondary return. By viewing the four operation scenarios of Fig. 8, it follows that operation scenario 1 and 3 produce different scenarios than what is used to measure the asymmetrical and symmetrical models equivalent circuit parameters. Operation scenario 2 is however the same as the measurement used to define C_{12}, while operation scenario 4 is a state of zero impedance. For this reason, operation scenarios 1 and 3 are used for comparing the asymmetrical

TABLE II
IMPEDANCE EQUATIONS OF THE TWO TRANSFORMER MODELS

	Symmetrical model	Asymmetrical model
Scenario 1	$Z_{sym,S1} = \dfrac{sL_m}{s^2L_m\left(C_1 + n^2C_2 + \frac{1}{4}C_{12}\,(1-n)^2\right) + 1}$	$Z_{asym,S1} = \dfrac{sL_m}{s^2L_m\left(C_1 + n^2C_2 + C_{12}\,(1-n)^2\right) + 1}$
Scenario 3	$Z_{sym,S3} = \dfrac{sL_m}{s^2L_m\left(C_1 + n^2C_2 + \frac{1}{4}C_{12}\,(1-n)^2\right) + 1}$	$Z_{asym,S3} = \dfrac{sL_m}{s^2L_m\left(C_1 + n^2C_2\right) + 1}$

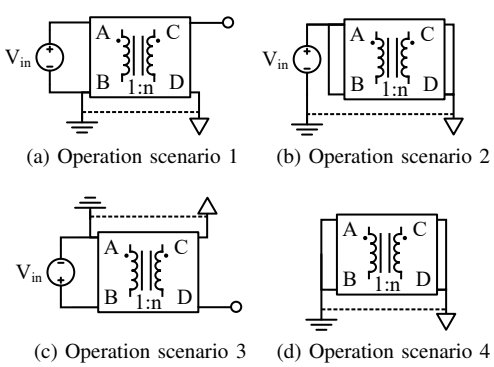

(a) Operation scenario 1 (b) Operation scenario 2

(c) Operation scenario 3 (d) Operation scenario 4

Fig. 8. Illustration of the transformer connections during the operation scenarios of an isolated full bridge phase-shift DC-DC converter

and symmetrical model.

In [8] it is shown that operation scenario 1 and 3 are used to define the parameters of six-capacitor model. Since measurements that are used for parameter extraction always matches the measured impedance, will the six-capacitor model not be compared with the symmetrical model. If the impedance of the six-capacitor model are to be compared with symmetrical model, it should be in a scenario that are not used for parameters extraction.

A. Transformer impedance in the operation scenarios

The impedance equations of operation scenarios 1 and 3 in the symmetrical model is different compared to those of the asymmetrical model. The impedance equation of operation scenario 1 for the symmetrical model is derived from Fig. 9, which illustrates the effective circuit during the scenario. The input current of the model (I_{in}) is expressed as

$$I_{in} = I_{C_1} + I_{L_m} + I_{p1} \tag{8}$$

All the current flowing to the ideal transformer primary side $(I_{p1} + I_{p2})$ are transformed to the secondary side $(I_{s1} + I_{s2})$ with the turns-ratio (n), therefore

$$I_{p1} + I_{p2} = n\ (I_{s1} + I_{s2}) \tag{9}$$

From Fig. 9 is it clear that

$$I_{p2} = I_{p1} - I_{C_{12}} \tag{10}$$

$$I_{s1} = I_{C_2} \tag{11}$$

$$I_{s2} = I_{C_2} - I_X = I_{s1} - I_{C_{12}} \tag{12}$$

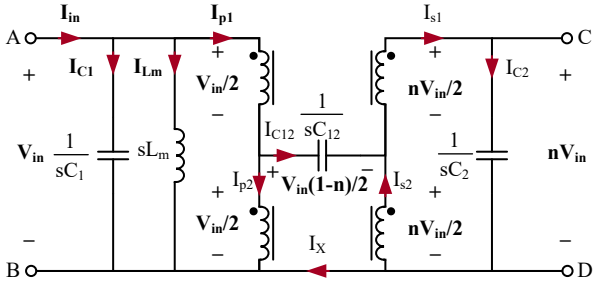

Fig. 9. Symmetrical transformer model in operation scenario 1

By comparing (11) and (12), it follows that $I_{C_{12}} = I_X$. Inserting (10), (11) and (12) in (9) yields

$$I_{p1} = n\,I_{C_2} + \frac{1}{2}\,I_{C_{12}}\,(1-n) \tag{13}$$

Thereafter by inserting (13) in (8) gives

$$I_{in} = I_{C_1} + I_{L_m} + n\,I_{C_2} + \frac{1}{2}\,I_{C_{12}}\,(1-n) \tag{14}$$

The impedance of each component are illustrated on Fig. 9 along with their corresponding voltage potential, where V_{in} is the voltage applied to the model. The admittance and impedance of operation scenario 1 are therefore as shown in (15) and (16) respectively.

$$\frac{I_{in}}{V_{in}} = s\,C_1 + \frac{1}{s\,L_m} + s\,C_2\,n^2 + \frac{1}{4}\,s\,C_{12}\,(1-n)^2 \tag{15}$$

$$Z_{sym,S1} = \frac{sL_m}{s^2L_m\left(C_1 + n^2C_2 + \frac{1}{4}C_{12}\,(1-n)^2\right) + 1} \tag{16}$$

The impedance of operation scenario 3 is derived the same way, and it yields the same result as in (16) when using the symmetrical model. The impedance of operation scenario 1 and 3 are also derived for the asymmetrical model by using the same method, and a comparison of the impedance equations among the two models are listed in Table II. It follows that the symmetrical model predicts the same impedance in operation scenario 1 and 3, whereas the asymmetrical model predicts different impedance. Only when the turns-ratio equals 1 does the two models predict the same impedance in both operation scenarios.

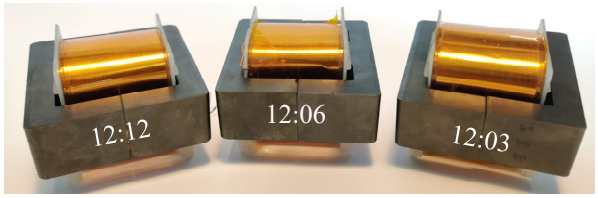

Fig. 10. Three constructed foil transformers

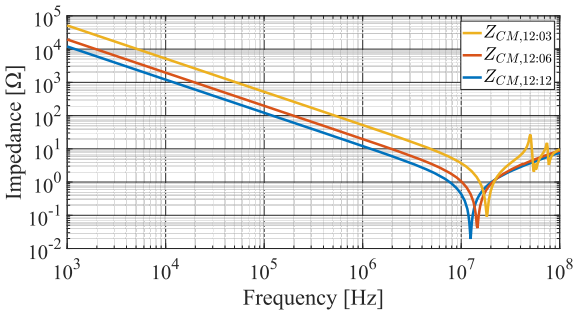

(a) Interwinding measurement, Z_{CM}

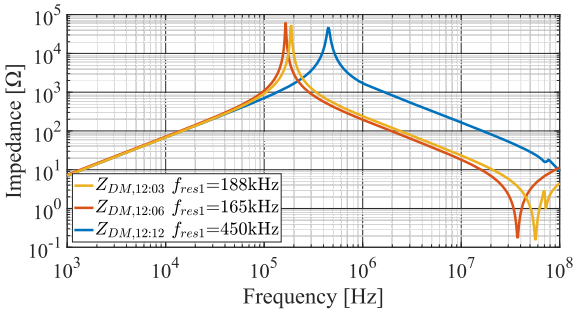

(b) Open circuit measurement seen from primary, Z_{DM}

Fig. 11. Measurement used for parameter extraction of the three transformers

V. Experimental Results

Three transformers with the same core but different turns-ratio are constructed. The utilized core is the E55/28/21-3C90 from Ferroxcube and the turns-ratios are 12:12, 12:06 and 12:03 respectively. The primary and secondary winding for each transformer are constructed by using copper foils of 0.15mm thickness and 30mm width. The primary and secondary winding of each transformer are heavily interleaved, to minimize AC resistance and leakage inductance [13], [15], [16]. The constructed transformers are shown on Fig. 10.

The equivalent circuit parameters of the transformers are measured by using a Keysight 4294A Precision Impedance Analyzer. The results are shown on Fig. 11. It follows from Fig. 11a that the three transformers all have a resonance frequency after 10Mhz. This resonance frequency is a product of C_{12} and the transformer parasitic inductance added with the termination inductance. The capacitor C_{12} dominates the impedance before the resonance, allowing for a simplified impedance equation as shown in (6). The measured C_{12} for the three transformers are listed in Table III.

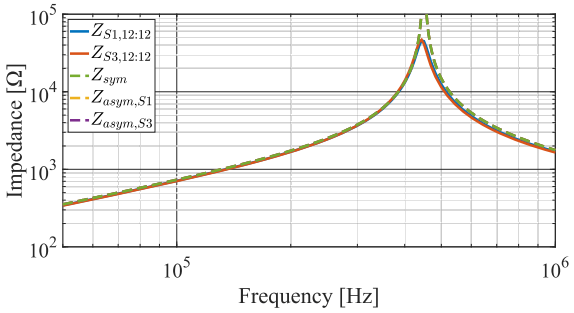

(a) Transformer turns-ratio 12:12

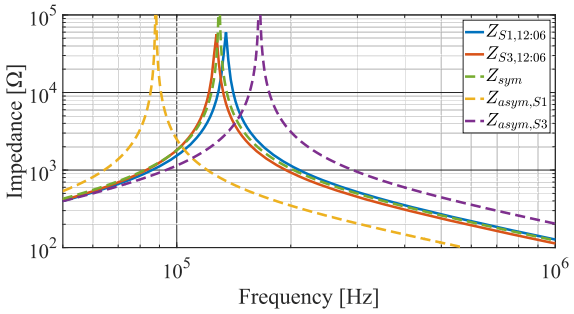

(b) Transformer turns-ratio 12:06

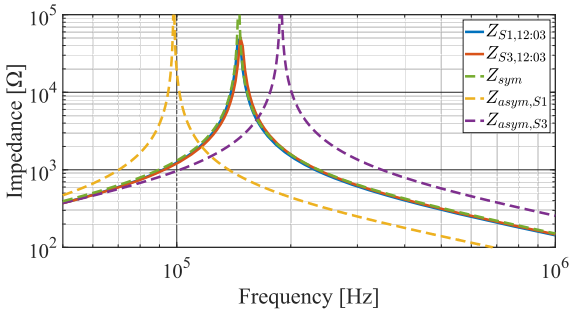

(c) Transformer turns-ratio 12:03

Fig. 12. The measured impedance (Z_{s1}) of the three transformers in operation scenario 1, compared with the theoretically calculated impedance of the asymmetrical and symmetrical transformer model

The measurement on Fig. 11b equals the impedance from (7). The numerical value of the first resonance frequency (f_{res1}) for each transformer is shown on the figure. The impedance before the resonance frequency is dominated by the magnetizing inductance (L_m), from which its value can be obtained. The equivalent capacitance value (C_{eq}) of the measurement are derived as shown below, and the values are listed in Table III.

$$C_{eq} = C_1 + n^2 C_2 = \frac{1}{4\pi^2 L_m \left(f_{res1}\right)^2} \tag{17}$$

Measurements of operation scenario 1 and 3 are performed on the transformers according to the depictions from Fig. 8. The impedance is measured from V_{in} in both scenarios, and a physical short are performed to mimic the virtual short. The measured impedance of operation scenario 1 (Z_{S1}) and 3 (Z_{S3}), together with the theoretical impedance equations

TABLE III
MEASURED TRANSFORMER EQUIVALENT CIRCUIT PARAMETERS

Turns-ratio	L_m	$C_1 + n^2C_2$	C_{12}
12:12	1.11 mH	113 pF	13.19 nF
12:06	1.15 mH	804 pF	8.13 nF
12:03	1.11 mH	646 pF	3.08 nF

TABLE IV
EQUIVALENT CAPACITANCE OF THE OPERATION SCENARIO 1

Turns-ratio	Measured	Symmetrical model	Asymmetrical model
12:12	115 pF	113 pF	113 pF
12:06	1223 pF	1312 pF	2837 pF
12:03	1104 pF	1079 pF	2377 pF

TABLE V
EQUIVALENT CAPACITANCE OF THE OPERATION SCENARIO 3

Turns-ratio	Measured	Symmetrical model	Asymmetrical model
12:12	116 pF	113 pF	113 pF
12:06	1372 pF	1312 pF	804 pF
12:03	1073 pF	1079 pF	646 pF

from Table II, are compared on Fig. 12. Since the symmetrical model predicts the same impedance in both of the operation scenarios, it is chosen to present both of the predictions as Z_{sym}.

The measurement on Fig. 12a shows results of the transformer with turns-ratio 12:12. The impedance equation in Table II show that when the turns-ratio equals one ($n = 1$) both models predict the same result, which is evident from Fig. 12a. The small difference between the measurement and calculation is due to non-ideal connections. The measurement of the transformer with turns-ratio 12:06 and 12:03 are shown in Fig. 12b and 12c, respectively. The comparison between the measurement and the models clearly shows that only the symmetrical model provides the correct results for the operation scenarios.

The equivalent capacitance value of each of the measurements are derived using (17), and the numeric values for operation scenario 1 and 3 are listed in Table IV and V respectively, along with the equivalent capacitance of the model predictions. It follows that for turns-ratios different from one, the asymmetrical model has an error of 40%-132%, whereas the symmetrical model only has an error of 0.6%-7.3%. The large error of the asymmetrical model proves that it provides faulty analysis of e.g. the capacitive power loss or emitted noise of the transformer. Only the symmetrical model provides accurate analysis of the transformer behavior for all turns-ratios.

VI. CONCLUSION

A new symmetrical transformer equivalent circuit model has been proposed and compared to a commonly used asymmetrical model. It has been shown how the operation of a isolated full bridge phase-shift DC-DC converter, subject the transformer to four different operation scenarios. Two of those scenarios are chosen to compare the two models. The proposed symmetrical model has been shown to accurately reflect the impedance in both scenarios, while the asymmetrical model does not.

Common-mode and differential-mode signals in a transformer has been explained. It has been described that the symmetrical model clearly separates which lumped capacitors are influenced by common-mode and differential-mode signals, whereas other equivalent circuit models does not. The symmetrical model does therefore allow for a simpler analysis of the common-mode and differential-mode noise than other model does.

Three heavily-interleaved foil transformers was constructed with different turns-ratio, and their equivalent circuit parameters were extracted. The three transformers were subjected to the operation scenarios, and the measured results were compared to the calculated response from the models. It was shown that both models provided correct impedance prediction for turns-ratio equal to one. For turns-ratios different from one, the asymmetrical model had an error of 40%-132% in the predicted equivalent capacitance of the measurements, whereas the symmetrical model only had errors between 0.6%-7.3%. The symmetrical model is therefore the only model that predicts accurate transformer behavior for any turns-ratio.

ACKNOWLEDGMENT

The project is supported by the Innovation Fund Denmark under the project Advanced Power Electronic Technology and Tools (APETT), strategic research project between the industries and universities.

REFERENCES

[1] I. A. Makda and M. Nymand, "Common mode noise generation and filter design for a hard switched isolated full-bridge forward converter," in *IECON 2014 - 40th Annual Conference of the IEEE Industrial Electronics Society*. IEEE, oct 2014.

[2] I. A. Makda and M. Nymand, "Common-mode noise analysis, modeling and filter design for a phase-shifted full-bridge forward converter," in *2015 IEEE 11th International Conference on Power Electronics and Drive Systems*, 2015, pp. 1100–1105.

[3] D. Bortis, G. Ortiz, J. W. Kolar, and J. Biela, "Design procedure for compact pulse transformers with rectangular pulse shape and fast rise times," *IEEE Transactions on Dielectrics and Electrical Insulation*, vol. 18, no. 4, pp. 1171–1180, aug 2011.

[4] Z. Ouyang, O. C. Thomsen, and M. A. E. Andersen, "Optimal design and tradeoff analysis of planar transformer in high-power DC–DC converters," *IEEE Transactions on Industrial Electronics*, vol. 59, no. 7, pp. 2800–2810, jul 2012.

[5] Hai Yan Lu, Jian Guo Zhu, and S. Y. R. Hui, "Experimental determination of stray capacitances in high frequency transformers," *IEEE Transactions on Power Electronics*, vol. 18, no. 5, pp. 1105–1112, sep 2003.

[6] "IEEE Recommended Practice for Testing Transformers and Inductors for Electronics Applications," *IEEE Std 389-2020 (Revision of IEEE Std 389-1996)*, pp. 1–97, 2020.

[7] A. Baccigalupi, P. Daponte, and D. Grimaldi, "On a circuit theory approach to evaluate the stray capacitances of two coupled inductors," *IEEE Transactions on Instrumentation and Measurement*, vol. 43, no. 5, pp. 774–776, 1994.

[8] B. Cogitore, J. P. Keradec, and J. Barbaroux, "The two-winding transformer: an experimental method to obtain a wide frequency range equivalent circuit," *IEEE Transactions on Instrumentation and Measurement*, vol. 43, no. 2, pp. 364–371, apr 1994.

[9] L. Dalessandro, F. da Silveira Cavalcante, and J. W. Kolar, "Self-capacitance of high-voltage transformers," *IEEE Transactions on Power Electronics*, vol. 22, no. 5, pp. 2081–2092, sep 2007.

[10] M. A. Saket, M. Ordonez, and N. Shafiei, "Planar transformers with near-zero common-mode noise for flyback and forward converters," *IEEE Transactions on Power Electronics*, vol. 33, no. 2, pp. 1554–1571, feb 2018.

[11] T. Duerbaum and G. Sauerlaender, "Energy based capacitance model for magnetic devices," in *APEC 2001. Sixteenth Annual IEEE Applied Power Electronics Conference and Exposition (Cat. No.01CH37181)*, vol. 1, 2001, pp. 109–115 vol.1.

[12] R. Prieto, R. Asensi, J. A. Cobos, O. Garcia, and J. Uceda, "Model of the capacitive effects in magnetic components," in *Proceedings of PESC '95 - Power Electronics Specialist Conference*, vol. 2, 1995, pp. 678–683 vol.2.

[13] M. Nymand and M. A. E. Andersen, "High-efficiency isolated boost DC–DC converter for high-power low-voltage fuel-cell applications," *IEEE Transactions on Industrial Electronics*, vol. 57, no. 2, pp. 505–514, feb 2010.

[14] R. Ramachandran and M. Nymand, "Design and analysis of an ultra-high efficiency phase shifted full bridge gan converter," in *2015 IEEE Applied Power Electronics Conference and Exposition (APEC)*, 2015, pp. 2011–2016.

[15] R. Ramachandran and M. Nymand, "Experimental demonstration of a 98.8% efficient isolated DC–DC GaN converter," *IEEE Transactions on Industrial Electronics*, vol. 64, no. 11, pp. 9104–9113, nov 2017.

[16] R. Ramachandran, M. Nymand, C. Østergaard, C. Kjeldsen, and G. Kapino, "High efficiency 20kw sic based isolated dc-dc converter for battery charger applications," in *2018 20th European Conference on Power Electronics and Applications (EPE'18 ECCE Europe)*, 2018, pp. P.1–P.9.